STUDY OF FORCE PARAMETERS OF FLEXIBLE SCREW CONVEYOR DURING TRANSPORTATION OF EXCAVATED CONTAMINATED SOIL FROM CRATER CENTER

Oleksandra Trokhaniak[1], Myroslav Budzanivskyi[2], Volodymyr Martyniuk[1], Aivars Aboltins[3], Adolfs Rucins[3]

[1]National University of Life and Environmental Sciences of Ukraine, Ukraine; [2]Institute of Mechanics and Automatics of Agroindustrial Production of the National Academy of Agrarian Sciences of Ukraine, Ukraine; [3]Latvia University of Life Sciences and Technologies, Latvia
klendii_o@ukr.net, aivars.aboltins@lbtu.lv, adolfs.rucins@lbtu.lv

Abstract. This article presents a design diagram of the experimental setup, developed to investigate the effect of structural and kinematic parameters on the torque at the drive shaft during the soil transportation from the center of the crater. The research was conducted varying the screw rotation speed, the lifting height of the excavated soil, and the radius of curvature of the flexible screw-type sectional working body. Based on the conducted studies, corresponding regression equations and response surfaces were constructed to investigate the influence of the specified parameters on the torque value on the drive shaft during transport. The analysis of the obtained regression equation established that the dominant factor influencing the torque value is the material lift height *h*. It was also determined that the radius of the curvature *R* of the flexible screw-type sectional working body has a significant influence on the torque value. The least influential factor on the torque is the rotational speed *n* of the working body.

Keywords: flexible screw conveyor, transport, torque, sinkhole, contaminated soil.

Introduction

All the forms of military and man-made impact lead to severe contamination and degradation of the soil cover. The effects of all munitions, used in military operations, are that they cause shock waves and create products of explosion that spread into the surrounding environment.

First and foremost, the soil deformation occurs in all directions of the shock wave propagation. As a result of combustion, explosion and detonation of munitions, various by-products are created, most of which are either toxic or hazardous pollutants.

The internal components of the soil are scattered over significant area. The soil remaining within the blast zone undergoes intense turbulence and dynamic compaction and is characterized by the presence of numerous metal fragments containing residues of toxic explosives [1-3].

These damages are visible to the naked eye; however, to determine the chemical impact, an analysis must be conducted, as the impact is caused by a thermal pulse, explosion, and soil disturbance. This also disrupts the soil's biological structure. Craters from detonations and the surrounding area, depending on the debris scattering radius, are contaminated with toxic metals (nickel, zinc, lead, cadmium, copper, etc.). During the detonation of rockets and aerial bombs, it is not only the air that becomes contaminated. Hazardous substances do not remain in the atmosphere for long but return in the form of precipitation and accumulate in the soil. The toxic elements may penetrate through the soil into water or the plants grown on it; these pollutants may migrate in the environment and accumulate in the organisms of the plants and animals [4-6]. The heavy metals are present in all munitions; they accumulate in the top 10 cm of soil and are biologically available to the surrounding ecosystems. During high-intensity detonations, small metal fragments from projectiles scatter over varying distances depending on their explosive power and in accordance with the blast radius. Incomplete detonations scatter the largest parts of the shell casing [7; 8]. The work [9] presented that acidic and alkaline buffering capacities were most severely reduced in the topsoil layers, following the FPV drone strikes, highlighting increased vulnerability of these soils to further chemical stressors. An X-ray fluorescence analysis revealed significantly elevated levels of potentially toxic metals (Pb, Zn, Cu, Cr, Co, As) in combat-impacted soils, providing clear evidence of anthropogenic contamination, derived from explosive residues and military munitions.

Analysis of the soil samples taken directly from the crater and from the area of impact on the soil cover after combat operations revealed that concentrations of cadmium, chromium, and lead were recorded in the craters (in craters from 120-125 mm munitions, cadmium concentration factors are approximately 4-17 clarks above background levels; 82 mm munitions – 4 clarks; 152-155 mm shells – 2-18 clarks; and aerial bombs – 5-13 clarks; lead concentration factors are approximately 4-22 clarks in

the impact zones of 120-125 mm munitions, 2.6-4 clarks for 152-155 mm, 2.7 clarks for 82 mm munitions, and 2.7-11 clarks for aerial bombs). The maximum concentration of cadmium is observed on the crater slopes, while that of chromium is at the crater bottom. It should be noted that the type of munitions was determined either by debris near the crater or by the size of the crater [9].

Other significant impacts on the soil cover include the consequences of the explosion, detonation, or ignition of heavy equipment on agricultural lands. Analysis of granulometric composition of the soil revealed that in the areas where the heavy equipment ignited or fuel and lubricants leaked, the content of the physical clay decreased [10]. The consequences of contamination of natural resources through military activities, the disruption of critical ecosystems, and the subsequent threats for human health in living and future generations, are described in [10] review.

To assess the extent of the soil damage, it is necessary to determine the type and degree of contamination in each individual area. Based on these indicators, it is then necessary to establish the level of their suitability and the most efficient restoration methods. Some areas may be fully suitable and require only cleaning. Others, however, have sustained such damage that any activity will be impossible in the near future. In such cases, it is necessary to restore the topography of the agricultural land, level and recultivate it – that is, restore the optimal balance and fertility of the soil.

Reclamation of the damaged and contaminated land may be carried out mechanically. To do this, the craters must first be cleared of the damaged soil and the soil contaminated with heavy metals and other hazardous substances. After this, the craters must be backfilled, i.e. the surface levelled. Subsequently, the land can be harrowed and cultivated, and ploughed if necessary.

A screw conveyor with a flexible sectional working body can be employed to transport the cleared damaged soil from inside the crater. Since the use of articulated screw working elements ensures high efficiency in the loading and unloading processes when transporting loose agricultural materials along curved routes, improving the performance of screw conveyors is a pressing task.

Conveyors with screw working elements can be either stationary or mobile and are widely used for loading (transhipment) of bulk material into the bodies of lorries, railway wagons, ship holds, etc.

An analysis of the literature has revealed that the kinematic, dynamic, and design parameters of the working components, as well as their operating modes during the loading and overloading of bulk agricultural materials, have been studied for single- and double-screw conveyors [11-13], as well as during the material removal using active loading spouts [14].

The works [15; 16] present methods for determining the optimal parameters of the working elements of vertical and inclined screw conveyors, used for transporting agricultural materials.

Papers [17; 18] present a mathematical model of the flow of materials in a screw conveyor with a rotating casing. Of particular interest is the pneumatic screw-type flexible sectional conveyor [19], in which the conveying efficiency is enhanced by a directed flow of compressed air. This process captures fine particles and imparts additional conveying velocity to them; in effect, the particles are separated by size, shape, and mass. Using the methods described in [20], it is possible to conduct research, focused on the processes of grinding (milling) the entire soil mass to obtain a fine, homogeneous mass, as well as the pneumatic separation of the soil particles in a vortex flow.

In this regard, it will be important to improve and develop new designs for the working components of screw conveyors, determining their optimal kinematic, technological and structural parameters, which will improve the operational performance of the agricultural material transportation process.

Materials and methods

To determine the performance characteristics, a screw conveyor with a flexible sectional working body was developed, using which the laboratory studies were conducted on the transport of bulk material along curved paths for disposing of the soil contaminated from inside of the crater.

The experimental studies with the developed experimental setup were carried out using an Altivar 71 frequency converter and PowerSuite v.2.5.0 software to record the power parameters. Fig. 1 shows a schematic diagram of a flexible screw conveyor and the equipment used to control and obtain results for determining the kinematic parameters of the process.

To improve the performance of the process for transporting cleared, damaged soil, it is recommended to use the developed design of a flexible, sectional screw-type working body. Fig. 2 shows a general view of it.

The working element of the flexible screw conveyor consists of individual sections of identical diameter and length. Each section comprises rods 1 (each section contains two rods), to one end of which a cylindrical sleeve with a concave surface 2 is rigidly attached, along with a spherical pin and balls, for which there are three axial parallel grooves in the sleeve 2, which are evenly spaced around the circumference and engage with the balls. The balls of sleeve 2 also interact with the recesses of the pin. This ball-and-socket connection of the cylindrical sleeve 2 with a concave surface allows for its axial movement and angular rotation.

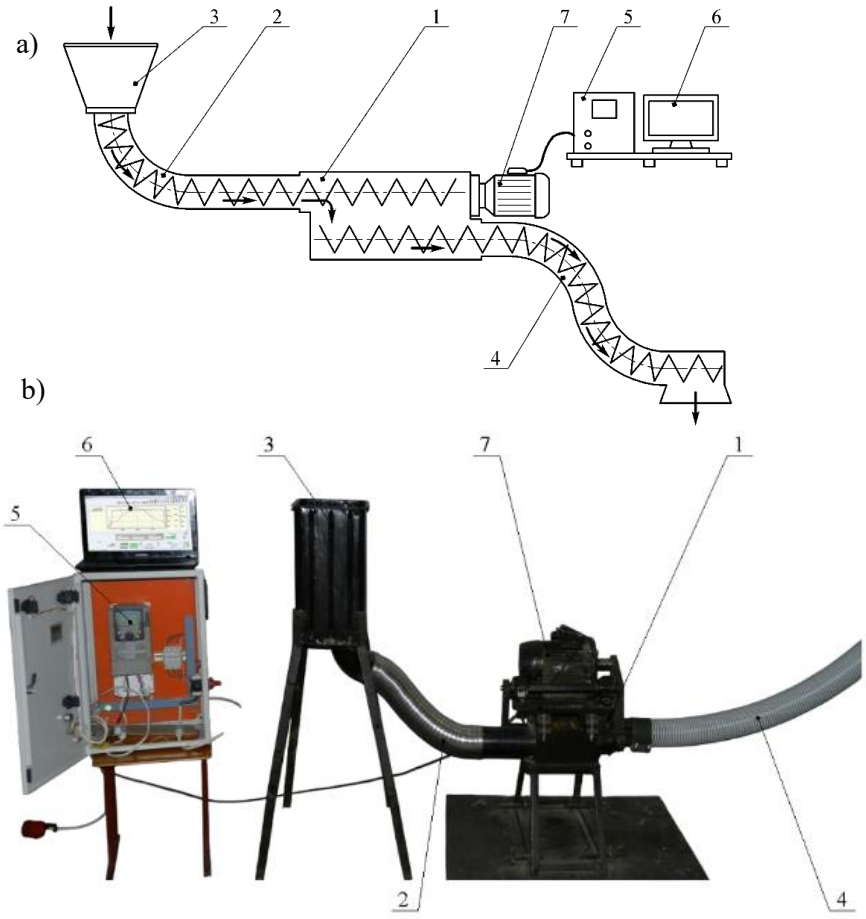

Fig. 1. **Schematic diagram (a) and general view (b) of a flexible screw conveyor and equipment for regulating the rotational speed of the electric motor rotor and obtaining results:** 1 – transfer unit; 2 – feed chute with a flexible fixed casing and a screw conveyor; 3 – soil hopper; 4 – discharge chute with a flexible fixed casing and a screw conveyor; 5 – Altivar 71 frequency converter; 6 – computer; 7 – conveyor drive motor

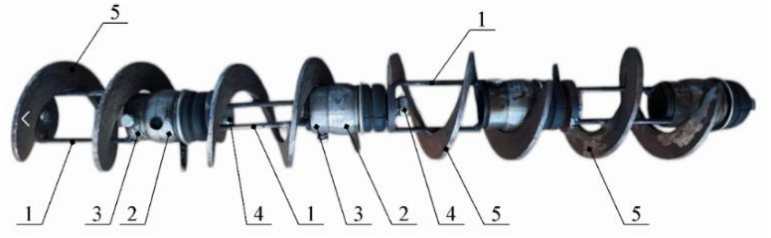

Fig. 2. **Schematic diagram (a) and general view (b) of the flexible screw sectional working body:** 1 – rods (2 pcs.) for each section; 2 – cylindrical bushing with a concave spherical surface, a spherical pin, and balls; 3 – connecting bushing; 4 – bolted joint; 5 – helical coil for each section

On the other side of rods 1, a connecting sleeve 3 is rigidly mounted in the inner bore of the section, perpendicular to its axis. It contacts the corresponding end of the finger of the cylindrical sleeve with a concave surface 2 of the adjacent section and is secured by means of a bolted connection 4. A helical coil 5 is welded to the outer surface of each cylindrical section.

The screw-type working element operates as follows. The screw spiral 5 of the section of the screw rotates, and the torque is transmitted to the pin via the balls in the cylindrical sleeve with a concave surface 2, and then on to the adjacent sections of the screw-type working element.

The experimental procedure was as follows. During the experimental studies, the loose soil was fed through the hopper into the loading chute, which consisted of a stationary flexible casing and a specially designed screw conveyor; the rotation of the screw conveyor moved the material toward the transfer pipe of the conveyor. Then the soil entered the discharge chute, which also contained a flexible casing and a screw conveyor that transported the material to the discharge zone.

The aim of the laboratory studies was to investigate the influence of the screw rotation speed, the lifting height of the excavated soil and the radius of curvature of the flexible sectional screw-type working body on the torque of the drive shaft during transport.

For the study, loose soil was collected from the experimental field of the Institute of Mechanics and Automation of Agro-Industrial Production at the National Academy of Agrarian Sciences of Ukraine. Loamy soil with a moisture content of 10-20% was used for this purpose.

The experiments were conducted with the conveying line fully filled with soil. To vary the rotational speed of the working body, a frequency converter was applied to adjust the frequency of the voltage, supplied to the motor/engine. The experimental investigations were conducted with a material transport line 4 m long, the lifting height of the scraped damaged soil layer was varied by changing the inclination angle of the line, and the radius of curvature of the flexible screw-type sectional working body was adjusted by altering the curvature of the process line.

To ensure a reliable assessment of the performance of the experimental setup during the research, the required number of repetitions was achieved with three replicates. To determine the influence of the independent factors on the transportation torque of the flexible screw conveyor under investigation, a comparative multifactorial experiment of the PFE-3^3 type was made. The dependence of the torque on the changes was determined in three factors. These factors included the screw rotation speed n, the lift height of the loose soil h, and the radius of curvature of the flexible helical articulated-section working element R. In other words, the relationship was determined $T = f(n, h, R)$.

Since during the experiments the independent variables are heterogeneous and have different units of measurement, and the numbers expressing the values of these factors are of different orders of magnitude, they were brought into a single system of calculations by converting from actual values to coded values. When coding the factors, the factor space is linearly transformed – the origin of the coordinate system is shifted to the center of the experiment, and the scale along the axes is chosen in units of factor variation [20].

Next, we constructed a design matrix for 3^3 PFE-type multifactorial experiment for a total number of trials $N = 3^3$, assigning coded values to the levels of variation for each factor: the upper level was designated as "+1", the lower level as "–1" and the zero level as "0". The results of coding the factors and their levels of variation are presented in Table 1.

Table 1

Results of factor coding and their levels of variation

Factors	Designation		Interval of variation	Levels of variation, natural/coded		
	Code	Natural				
Screw rotation frequency n, rpm	X_1	x_1	200	300/–1	500/0	700/+1
Soil lifting height h, m	X_2	x_2	1.0	1/–1	2/0	3/+1
Radius of curvature of the screw R, m	X_2	x_2	0.6	0.3/–1	0.9/0	1.5/+1

The factors of the continuous variables were coded based on the data in Table 1.

$$\left.\begin{aligned} X_1 &= 0.005 \cdot n - 2.5 \\ X_2 &= h - 1 \\ X_3 &= 1.67 \cdot R - 1.5 \end{aligned}\right\}. \quad (1)$$

After coding the factors, a design matrix was created for the corresponding 3×3 factorial experiment, with a total of $N = 3^3$ trials. These are shown in Table 2.

Table 2

Randomised design matrix for the 33PFE-type experiment

Experiment No.	Levels of factors				Interaction of factors			Optimisation parameter, *T*, Nm			Average values of T_s, Nm
								Repeatability			
	x_0	x_1	x_2	x_3	x_1x_2	x_1x_3	x_2x_3	1	2	3	
1	+ 1	–1	–1	–1	+ 1	+ 1	+ 1	20.25	22.29	22.30	21.61
2	+ 1	+ 1	–1	–1	–1	–1	+ 1	23.73	23.68	24.69	24.03
3	+ 1	0	–1	–1	0	0	+ 1	22.57	23.48	22.54	22.86
4	+ 1	–1	+ 1	–1	–1	+ 1	–1	24.07	29.10	29.14	27.44
5	+ 1	+ 1	+ 1	–1	+ 1	–1	–1	29.49	29.52	30.58	29.86
6	+ 1	0	+ 1	–1	0	0	–1	28.37	28.36	28.34	28.36
7	+ 1	–1	0	–1	0	+ 1	0	24.21	25.17	25.18	24.85
8	+ 1	+ 1	0	–1	0	–1	0	27.55	26.66	26.62	26.94
9	+ 1	0	0	–1	0	0	0	28.42	24.51	24.49	25.81
10	+ 1	–1	–1	+ 1	+ 1	–1	–1	29.63	29.61	29.56	29.60
11	+ 1	+ 1	–1	+ 1	–1	+ 1	–1	32.98	32.05	33.02	32.68
12	+ 1	0	–1	+ 1	0	0	–1	27.90	27.86	37.78	31.18
13	+ 1	–1	+ 1	+ 1	–1	–1	+ 1	36.49	36.45	34.34	35.76
14	+ 1	+ 1	+ 1	+ 1	+ 1	+ 1	+ 1	37.98	38.93	38.82	38.58
15	+ 1	0	+ 1	+ 1	0	0	+ 1	37.75	36.72	36.83	37.10
16	+ 1	–1	0	+ 1	0	–1	0	30.70	30.86	30.83	30.80
17	+ 1	+ 1	0	+ 1	0	+ 1	0	30.78	30.77	40.73	34.09
18	+ 1	0	0	+ 1	0	0	0	29.54	39.49	29.50	32.84
19	+ 1	–1	–1	0	+ 1	0	0	22.45	22.41	32.46	25.77
20	+ 1	+ 1	–1	0	–1	0	0	23.66	23.70	33.71	27.02
21	+ 1	0	–1	0	0	0	0	24.84	24.85	34.81	28.17
22	+ 1	–1	+ 1	0	–1	0	0	23.74	23.78	33.69	27.07
23	+ 1	+ 1	+ 1	0	+ 1	0	0	29.42	39.53	29.58	32.84
24	+ 1	0	+ 1	0	0	0	0	26.55	26.57	36.51	29.88
25	+ 1	–1	0	0	0	0	0	27.69	25.40	35.42	29.50
26	+ 1	+ 1	0	0	0	0	0	27.74	27.78	37.83	31.12
27	+ 1	0	0	0	0	0	0	26.62	26.66	36.51	29.93

During the implementation of the designed matrices, in order to eliminate the influence of the uncontrolled and unregulated factors on the experimental results, in particular on the torque values during transportation, the order of experiments was randomised. The randomisation of the design matrix was performed using the randomised block design method, which was implemented by randomly drawing the serial numbers of the trials from a box [20].

The experimental data, obtained following the planned experiments, were processed using well-known statistical methods and techniques, including correlation and regression analysis, to ultimately derive empirical regression equations. The optimization parameter, i.e. the torque $T = f(n, h, R)$, determined experimentally, was sought in the form of a mathematical model of a well-known quadratic polynomial [20].

The reproducibility of the values, obtained from the experimental data set, with an identical number of repetitions for each experiment, was tested using Cochran's criterion.

$$G = \frac{S_{v\max}^2}{\sum_{u=1}^{n} S_v^2}, \quad (2)$$

where G – calculated value of the Cochran criterion;
$S_{v\,max}$ – numerical value of the maximum variance at the u-th point;
S_v – variance characterising the dispersion of the results of the u-th experiment.

After performing the calculations using the formulas, it was established that the calculated value of the Cochran criterion is $G = 0.05436$. The calculated values of the Cochran criterion were compared with the tabulated value $G_T = 0.245$ at a confidence level of $\alpha = 0.05$. The condition $G \leq G_T$ is satisfied, and the variances are considered homogeneous, which means that the process is reproducible.

The response function (optimisation parameter), i.e. the torque $T = f(n, h, R)$, determined experimentally, was modelled using a well-known quadratic polynomial:

$$T = b_0 + b_1x_1 + b_2x_2 + b_3x_3 + b_{12}x_1x_2 + b_{13}x_1x_3 + b_{23}x_2x_3, \quad (3)$$

where $b_0, b_1, b_2, b_3, b_{12}, b_{13}, b_{23}$ – coefficients of the corresponding values x_i;
x_1, x_2, x_3 – corresponding coded factors.

The statistical significance of the regression equation coefficients $b_{i(jk)}$ was determined using Student's t-test [20].

The coefficients of the approximating polynomial were determined using the corresponding general formulas [20].

The free term b_0 and the coefficients $b_{0,}\ i$ of the factor:

$$b_i = \frac{\sum_{u=1}^{N} x_{iu}\bar{y}_u}{\sum_{u=1}^{N} x_{iu}^2} = \frac{\sum_{u=1}^{N} x_{iu}\bar{y}_u}{N}, \quad (4)$$

The interaction coefficients b_{ij}:

$$b_{ij} = \frac{\sum_{u=1}^{N} x_{iu}xju\bar{y}_u}{N}, \quad (5)$$

where x_{iu}, x_{ju}, x_{ku} – values of the coded variable in the corresponding column of the experimental design;
$\bar{y}_u$ – mean result of the u-th experiment;
u – serial number of the experiment;
i – factor number;
j, k – factor number, other than the i-th;
N – number of experiments conducted.

If the significance condition was not met, then such coefficient $b_{i(jk)}$ of the regression equation was considered insignificant (equal to zero), and the corresponding term $x_{(i)}$ of the regression equation was excluded.

The values of the regression equation coefficients are presented in Table 3.

Table 3

Values of the regression equation coefficients

b_0	b_1	b_2	b_3	b_{12}	b_{13}
29.5021	2.2452	3.2801	0.9322	0.8889	−0.8967

Thus, we obtain the regression equation:

$$T = 29.5021 + 2.2452 \cdot x_2 + 3.2801 \cdot x_3 + 0.9322 \cdot x_1 \cdot x_2 - 0.8967 \cdot x_2 \cdot x_3 + 0.88896 \cdot x_1 \cdot x_3\,. \quad (6)$$

The adequacy of the selected mathematical model was tested against experimental data – that is, the correspondence of the model to the real-world process – using the Fisher criterion (F) as follows.

The adequacy variance was determined:

$$S_{ag}^2 = \frac{m}{N-g'} \sum_{u=1}^{N} \left(\overline{Y}_u - \widetilde{y}_u\right)^2 , \quad (7)$$

where $N - g'$ – number of degrees of freedom of the adequacy variance;
g' – number of significant coefficients in the regression equation;
$\overline{Y}_u$ – mean response value in the u-th experiment;
$\widetilde{y}_u$ – response value at the u-th point of the plan, calculated using the regression equation.

The calculated Fisher's exact test statistic was determined as F_p:

$$F_p = \frac{S_{ag}^2}{S^2(Y)}, \quad (8)$$

where $S^2(Y)$ – replication variance of the experiment.

We determined the tabulated value of the Fisher's criterion F_T at a specified significance level α and two degrees of freedom [20]: $f_{ag} = N - g$ and $f_y = N(n - 1)$.

The adequacy of the selected mathematical model was tested according to the condition $F_p < F_T$. The obtained value F_p was compared with the tabulated value F_T. If the condition is satisfied, then the PFE regression equation is adequate to the experimental data.

The calculated value of the Fisher criterion is $F_p = 1.3089$, and, accordingly, $F_T = 1.93$ at a 5% significance level. Therefore, the condition of adequacy of the selected mathematical model is satisfied, i.e. the PFE regression equation is consistent with the experimental data.

Next, the multiple correlation coefficient was also determined using the formula

$$R = \sqrt{1 - \frac{\sum_{u=1}^{N} \left(\overline{Y}_u - \widetilde{y}_u\right)^2}{\sum_{u=1}^{N} \left(\overline{Y}_u - \overline{Y}\right)^2}}, \quad (9)$$

where $\overline{Y}$ – mean value of the function, determined from the experimental data.

The value of the multiple correlation coefficient is $R = 0.987$.

Thus, the general form of the regression equation in natural coordinates for the torque on the drive shaft during transport by a flexible screw conveyor, after transformation and simplification of the expressions, takes the form:

$$T = 25.2572 - 0.0114 \cdot n + 1.2598 \cdot h + 3.2641 \cdot R + 0.0047 \cdot n \cdot h - 1.4975 \cdot h \cdot R + 0.0075 \cdot n \cdot R . \quad (10)$$

The resulting regression equation (10) can be used to determine the torque as a function of the screw rotation speed, n, the soil lift height, h, and the screw curvature radius, R, within the following ranges of input factors: $300 \le n \le 700$ (rpm); $0.3 \le R \le 1.5$ (m); $1 \le h \le 3$ (m).

Results and discussion

Based on calculations, performed using the "Statistica 13.0" statistical software package for processing and analysing the results of experimental studies, three-dimensional response surfaces were constructed showing the dependence of the torque on the drive shaft during the material transportation by a flexible screw conveyor, as well as their two-dimensional cross-sections. This made it possible to visually present the results of the laboratory experimental studies and analyse the influence of individual factors and their interaction on the optimisation parameter, i.e. $T = f(n, h, R)$.

Fig. 3 shows the response surfaces of the torque on the drive shaft during transportation by a flexible screw conveyor and their two-dimensional cross-sections as a function of two variable factors $x_{i\,(1,2)}$ at a constant level of the corresponding third factor $x_{i\,(3)}$ = const. To examine the value of the third factor, a value equal to the factor's value at the zero level was selected.

The analysis of the regression equation shows that the dominant factor, influencing the torque, is the material lift height h. The radius of curvature R of the flexible screw section of the working element also has a significant influence on the torque. The least influential factor is the rotational speed n of the working element.

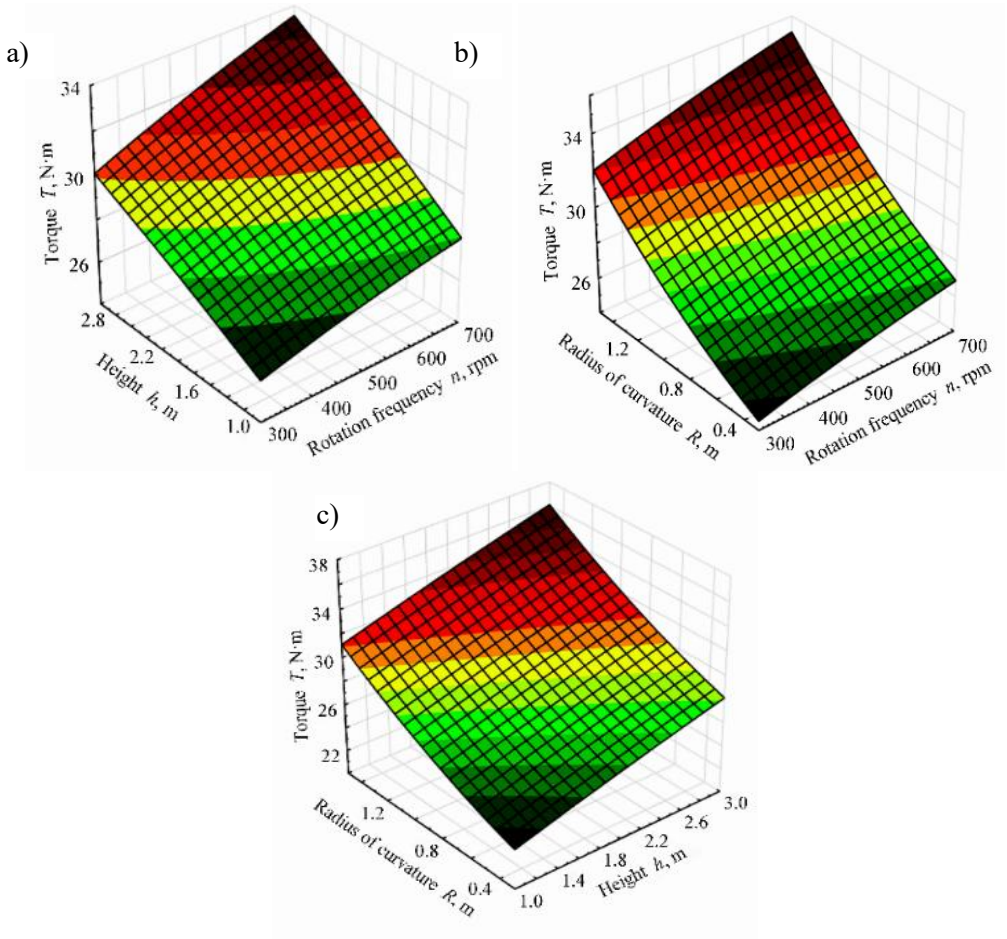

Fig. 3. **Response surfaces for changes in the torque on the drive shaft during transportation by a flexible screw conveyor:** a – $T = f(n; h)$; b – $T = f(n; R)$; c – $T = f(h; R)$

When the material lift height h varies within the range of 1-3 m, the torque increases by 18%; when the radius of curvature of the screw R varies within the range of 0.3-1.5 m, the torque increases by 14%, and when the rotational speed of the working element n varies from 300 rpm to 700 rpm, the torque increases by 10.5%.

Conclusions

1. This article presents the design diagram of a newly developed experimental flexible screw conveyor system, which enables the study of the transportation of bulk material along curved paths for the disposal of loose, contaminated soil, excavated from the center of a crater formed by explosions. When transporting the excavated contaminated soil, it is recommended to use the developed design of a flexible sectional screw conveyor.
2. A methodology has been developed for conducting experimental studies of a screw conveyor with a flexible sectional screw.
3. A multi-factor experiment was conducted to investigate the influence of the screw rotation speed, the lifting height of the cleared soil, and the radius of curvature of the flexible screw-type sectional working body on the torque value.
4. From an analysis of the regression equation presented, it has been established that the dominant factor influencing the magnitude of the torque is the lifting height of the material h. The radius of the curvature R of the flexible screw-type sectional working element also has a significant impact on the variation in torque.
5. The least influential factor is the rotational speed n of the working body. When the material lift height h varies within the range of 1-3 m, the torque increases by 18%; when the radius of curvature of the screw R varies within the range of 0.3-1.5 m, the torque increases by 14%; and within the

range of the rotational speed n of the working element from 300 rpm to 700 rpm, the torque value increases by 10.5%.

Author contributions:

Investigation, O.T., A.A. and A.R., software, M.B., data curation. V.M. All authors have read and agreed to the published version of the manuscript.

References

[1] Rawtani D., Gupta G., Khatri N., Rao P.K., Hussain C.M. Environmental damages due to war in Ukraine: a perspective. Sci. Total Environ. 850, 2022, 157932. DOI: 10.1016/j.scitotenv.2022.157932

[2] Bonchkovskyi O., Ostapenko P., Bonchkovskyi A., Shvaiko V. War-induced soil disturbances in north-eastern Ukraine (Kharkiv region): Physical disturbances, soil contamination and land use change, Science of The Total Environment, 2025, Volume 964, 2025, 178594, ISSN 0048-9697, DOI: 10.1016/j.scitotenv.2025.178594

[3] Balyuk S.A., Kucher A.V., Solokha M.O., Solovey V.B., Smirnov K.B., Momot G.F., Levin A.Ya. The impact of armed aggression and military actions on the current state of the soil cover, assessment of damage and losses, restoration measures. Kharkiv: FOP Brovin O.V., 2022, 102 p. (In Ukrainian)

[4] Kaminsky V.F., Tkachenko M.A., and Kolomiets M.P. Methodological Recommendations for the Restoration of Agricultural Land Damaged by Military Operations. Kyiv: National Scientific Center "IAE.", 2023, 84 pp. (In Ukrainian)

[5] Rucins A., Kolomiiets L., Shevchenko I., Bulgakov V., Holovach I., Trokhaniak O., Kiernicki Z. Research of the systems of environmental and soil protection technologies in erosion-hazardous agrolandscapes. Journal of Ecological Engineering, 26 (4), 2025, pp. 15-27.

[6] Bulgakov V., Glazunova O., Holovach I., Trokhaniak O., Ruzhylo Z., Rucins A., Aboltins A., Popov G., Beloev I., Vasileva V. Investigation in Working Body Power Parameters and Energy Capacity for Removing Damaged Soil from Surface of Craters. Engineering for Rural Development, 24, 2025, pp. 139 – 146.

[7] Bennour E., Kezrane C., Kaid N., Alqahtani S., Alshehery S., Menni Y. Improving mixing efficiency in laminar-flow static mixers with baffle inserts and vortex generators: A three-dimensional numerical investigation using corrugated tubes. Chem. Eng. Process. Process Intensif. 2023, 193, 109530

[8] Kovrov O., Koveria A., Shemet V., Ovcharenko A., Cherdantseva K., Panteleieva O., Malichenko V. Ecological assessment of soil quality affected by the Shahed-136 drone strike: Case study in Kirovograd region, Ukraine. Sustainable Environment, 12 (1), 2026, art. no. 2615531, DOI: 10.1080/27658511.2026.2615531

[9] Bolshanina S., Krupska A., Szewczuk-Karpisz K., Yanovska G. Alterations of Physicochemical Soil Properties Induced by Military Explosions. Environmental Problems, 11 (1), 2026, pp. 101-110, DOI: 10.23939/ep2026.01.101

[10] Yutilova K., Shved E., Rozantsev G., Adamski A. Russia–Ukraine war impacts on environment: warfare chemical pollution and recovery prospects. Environmental Science and Pollution Research, 32 (10), 2025, pp. 5685-5702, DOI: 10.1007/s11356-025-36098-9

[11] Ivanovs S., Bulgakov V., Nadykto V., Ihnatiev Y., Smolinskyi S., Kiernicki Z. Experimental study of the movement controllability of a machine-and-tractor aggregate of the modular type. INMATEH - Agricultural Engineering, 61 (2), 2020, pp. 9-16, DOI: 10.35633/inmateh-61-01

[12] Trokhaniak O. M., Hevko R. B., Lyashuk O. L., Dovbush T. A., Pohrishchuk B. V., Dobizha N. V. Research of the of bulk material movement process in the inactive zone between screw sections. INMATEH - Agricultural Engineering, 60, (1), 2020, pp. 261-268.

[13] Lyashuk, O., Vovk, Y., Sokil, B., Klendii, V., Ivasechko, R., Dovbush, T. Mathematical model of a dynamic process of transporting a bulk material by means of a tube scraping () Agricultural Engineering International: CIGR Journal, 21 (1), 2019, pp. 74-81.

[14] Bulgakov V., Trokhaniak O., Adamchuk V., Chernovol M., Korenko M., Dukulis I., Ivanovs S. A Study of Dynamic Loads of a Flexible Sectional Screw Conveyor. Acta Technologica Agriculturae, 25 (3), 2022, pp. 131-136.
[15] Olt J., Bulgakov V., Trokhaniak O., Klendii M., Gadzalo I.A., Ptashnik M., Tkachenko M. Harrow with screw-type operating tools: Optimisation of design and process parameters. Agronomy Research, 20 (4), 2022, pp. 751-763.
[16] Aulin V.V., Pankov A.O., Zamota T.M., Lyashuk O.L., Hrynkiv A.V., Tykhyi A.A., Kuzyk, A.V. Development of mechatronic module for the seeding control system. INMATEH - Agricultural Engineering, 59 (3), 2019, pp. 1-8.
[17] Pneumatic screw sectional conveyor. Ukrainian Patent for Invention No. 130314 C2. Inventors: V.M. Bulgakov, O.M. Trokhanyak, et al. Published on January 14, 2026. Bulletin No. 2. (In Ukrainian).
[18] Bulgakov V., Holovach I., Bandura V., Ivanovs S. A theoretical research of the grain milling technological process for roller mills with two degrees of freedom. INMATEH – Agricultural Engineering, 52(2), 2017, pp. 99-106.
[19] Adamchuk V., Bulgakov V., Ivanovs S., Holovach I., Ihnatiev Y. Theoretical study of pneumatic separation of grain mixtures in vortex flow. Engineering for Rural Development, 2021, 20, pp. 657-664.
[20] Bulgakov V., Trokhaniak O., Adamchuk V., Olt J., Ivanovs S. Experimental Studies of Flexible Sectional Screw Conveyor Torque Value. Engineering for Rural Development, 21, 2022, pp. 472-477, DOI: 10.22616/ERDev.2022.21.TF164